Nonvesicular release of acetylcholine is required for axon targeting in the *Drosophila* visual system

Hong Yang and Sam Kunes*

Department of Molecular and Cellular Biology, Harvard University, Cambridge, MA 02138

Edited by Joshua R. Sanes, Harvard University, Cambridge, MA, and approved September 9, 2004 (received for review December 8, 2003)

We report evidence for a developmental role of acetylcholine in axon pathfinding in the *Drosophila* visual system. Acetylcholine was detected on photoreceptor axons during their navigation to target sites in the brain, a time well before the formation of functional synapses. The pattern of photoreceptor axon projections was severely disrupted when acetylcholine synthesis or metabolism was altered or eliminated, or when transgenic α-bungarotoxin, a nicotinic acetylcholine receptor antagonist, was expressed in the developing eye or brain. The requirement for acetylcholine signaling exists before photoreceptor neurons form synaptic connections and does not require the function of vesicular acetylcholine transporter protein. That this early effect of acetylcholine is mediated through nonvesicular release is further supported by the observation that transgenic expression of tetanus toxin, a blocker of neurotransmitter release via synaptic vesicles, did not cause similar photoreceptor axon projection defects. These observations support the notion that a form of acetylcholine secretion mediates the behavior of growth cones during axon pathfinding.

It has been generally thought that the release of neurotransmitter at axon terminals reflects synaptic activity and contributes to the development of synaptic connectivity via activity-dependent processes. However, a growing body of evidence suggests that neurotransmitters function in early development in processes that can be independent of synapses or synaptic activity, such as cell proliferation, differentiation, migration, axon outgrowth, and axon branching. In these roles, neurotransmitters are apparently released by mechanisms that are distinct from the conventional synaptic vesicular pathway (1, 2). For example, it has been shown that the neurotransmitters γ-aminobutyric acid and glutamate can be released in a Ca^{2+}- and soluble *N*-ethylmaleimide-sensitive factor attachment protein receptor-independent manner, before synapse formation (3).

The effects of loss of acetylcholine synthesis on branching patterns of motor axons is particularly interesting in light of the earlier observation that neurotransmitters may function as chemical signals in axon pathfinding. Experiments on isolated embryonic chick and *Xenopus* neurons (4, 5) and *Drosophila* CNS neurons (6) have indicated that the transmitter acetylcholine is synthesized very early in neural development and is present on growing axons well before they reach their target fields or establish functional synapses. Experiments in culture have supported the notion that acetylcholine may have a role in axon navigation. An acetylcholine gradient can cause a growth cone to change direction (7). These studies raise the possibility that nonsynaptic release of neurotransmitter might play a role in regulating growth cone behavior before synaptogenesis.

We have undertaken an investigation of the role of small molecule neurotransmitters in the development of the *Drosophila* visual system. In this system, light transduction depends on synthesis and delivery of the transmitter histamine by the photoreceptor neurons of the retina (8, 9). We show that transient developmental synthesis and local secretion of acetylcholine by photoreceptor axons is required for normal growth cone behavior. We provide evidence that this signal is transduced by nicotinic acetylcholine receptors (nAChR). These observations reveal a transient developmental role for a neurotransmitter that is independent of its function in synaptic transmission.

Materials and Methods

Immunohistochemistry. Staining was performed as described (10). Primary antibodies were used at the following dilutions: mouse anti-choline acetyltransferase (ChAT), 1:500; rabbit anti-acetylcholinesterase (AChE), 1:1,000; mouse anti-acetylcholine receptor (AChR) (Dα2), 1:100; mouse anti-AChR (ALS), 1:100; mAb24B10, 1:5; rabbit anti-Repo, 1:500; rat-anti-Elav, 1:20. A modified fixative (4% paraformaldehyde/0.5% glutaraldehyde) was used for rabbit anti-conjugated choline (ref. 11; Biogenesis, Bournemouth, U.K., 1:100; Gemac Society, Paris, 1:5,000). Secondary antibodies were used at the following dilutions: Cy3-donkey anti-mouse (Jackson), 1:100; Cy3-donkey anti-rabbit (Jackson), 1:500. Specimens were viewed on a Zeiss LSM510 confocal microscope.

Generation of Eye-Specific Mosaicism. Eye-specific mosaicism was generated by *eyeless-FLP*-induced mitotic recombination (12, 13). All specimens were raised at 25°C, except for cha^{ts2} and cha^{ts3}, which were raised at 18°C, 28°C, or 30°C. Specimens of the following genotypes were examined.

1. Mosaicism for cha^{ts2}, cha^{ts3}, ace^{J50}, ace^{j21}, and $vacht^{1}$ with positive *CD8-GFP* labeling and the *Minute* background, where *X* denotes any of the five mutations: *P[elav-GAL4] P[UAS-CD8GFP]/y,w; P[ey-FLP]/+; P[FRT] 82B, X/P[FRT] 82B, Minute P[tub-GAL80]*. For analysis of axon projections with marking restricted to photoreceptor neurons R3 and R4, *P[mδ-GAL4]]* (14) was used in place of *elav-GAL4*.
2. Mosaicism for cha^{ts2} in the *Minute* background without positive marking: *P[ey-FLP]/y, w; ; P[FRT] 82B,* cha^{ts2}*/P[FRT] 82B, Minute P[*w^{+}*]*.
3. Mosaicism for cha^{ts2} in the cell-lethal background, without positive marking: *P[ey-FLP]/y, w; ; P[FRT] 82B,* cha^{ts2}*/P[FRT] 82B, cl P[GMR-hid]*, where *cl* indicates a recessive mutation that causes cell lethality (13).

Ectopic Expression of α-Bungarotoxin (α-BGT). A synthetic α-BGT coding sequence (15) was cloned into the *pUAST* transformation vector (16). Transgenics were obtained and crossed to *GAL4* drivers *GMR-GAL4* (17), *ey-GAL4* (G. Rubin, University of California, Berkeley), or *P[mδ-GAL4]* (14), along with *P[UAS-CD8GFP]* to label the *GAL4* expressing cells. Third-instar larvae harboring both *GAL4* driver and the UAS-α-BGT transgenes were dissected and analyzed by immunohistochemistry.

This paper was submitted directly (Track II) to the PNAS office.

Abbreviations: AChR, acetylcholine receptor; nAChR, nicotinic AChR; α-BGT, α-bungarotoxin; AChE, acetylcholinesterase; ChAT, choline acetyltransferase; Vacht, vesicular acetylcholine transporter.

*To whom correspondence should be addressed. E-mail: kunes@fas.harvard.edu.

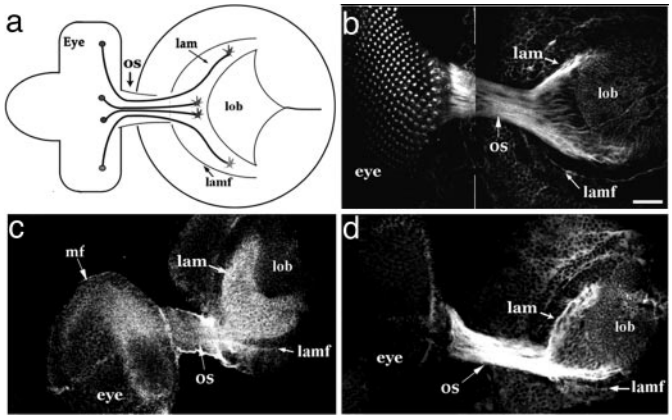

Fig. 1. Cholinergic phenotype of photoreceptor neurons during the establishment of axonal projections. (*a*) Schematic view of the third-instar larval visual system from a lateral perspective. Photoreceptor cells in the eye disk (eye) send their axons in ommatidial fascicles through the optic stalk (os) to retinotopic positions in the lamina (lam). The axons form a retinotopic map (dorsal is up). Posterior (right) to anterior retinotopic order in the lamina is established coincident with the neuron's temporal pattern of differentiation in the developing eye. The most recently arriving axons enter the lamina adjacent to a visible anterior landmark, the lamina furrow (lamf). (*b–d*) Retinal axons in the optic stalk (os) and lamina (lam) are specifically stained by antibodies against Ace (*b*), conjugated choline (*c*), and the nAChR subunit, Dα2 (*d*). In the case of conjugated choline staining, the antigen outlines the crescent-shaped pattern of photoreceptor axon projections, located adjacent to the lamina furrow (lamf). (Scale bar, 10 μm in *b*.)

Results

In the developing adult visual system of *Drosophila*, photoreceptor neurons form in ommatidial clusters as a wave of differentiation sweeps anteriorly across the eye imaginal disk in the third-instar larval stage. The photoreceptor axons converge at the posterior of the eye disk and traverse the optic stalk into the brain (Fig. 1*a*). In the brain, the axons encounter the prospective lamina and spread into a retinotopic pattern (18). Six (R1–R6) of the eight photoreceptor neurons of an ommatidium terminate extension in the lamina (Figs. 1*a* and 2 *a* and *e*) and, by the late pupal stage, establish an intricate pattern of synaptic connections there. The remaining two neurons, R7 and R8, project beyond the lamina into the medulla, where they likewise establish a precise retinotopic pattern (Fig. 2 *e* and *j*).

During the development of the *Drosophila* visual system, ChAT and AChE, which catalyze the synthesis and hydrolysis, respectively, of acetylcholine, are expressed by developing photoreceptor neurons and concentrated on their axons (Fig. 1*b*, refs. 19 and 20, and data not shown). The early cholinergic identity of photoreceptor neurons was further indicated by antibody staining against conjugated choline, which labeled their axons (Fig. 1*c*). Most intense antibody staining was detected in the lamina target field adjacent to the photoreceptor axon termini (Fig. 1*c*). The localization of intense immunofluorescence to the vicinity of photoreceptor axon termini, but not within axons, is consistent with the idea that acetylcholine is secreted and diffuses away from the axon termini. These observations indicate that acetylcholine is synthesized and metabolized in the visual system as photoreceptor axons arrive in their target region.

The *choline aceltyltransferase* (*cha*) and *acetylcholinesterase* (*ace*) genes were analyzed for requirements in visual system development. We examined temperature-sensitive mutants cha^{ts2} and cha^{ts3}, which are viable at the permissive temperature (18°C) where there is a relatively normal level of ChAT activity, and lethal at a restrictive temperature (30°C) where there is greatly diminished ChAT activity (21–23). We also examined the visual system in animals harboring the strong *ace* alleles, ace^{J21} or ace^{J50} (24, 25). AChE is required to hydrolyze acetylcholine, and thereby terminate impulse transmissions at cholinergic synapses (26). Mutation of *ace* might cause sustained signaling that leads to regulatory shut down of the pathway (25) or deplete the local supply of recycled choline and acetate necessary for acetylcholine synthesis. Our data, which reveal similar phenotypes in *ace* and *cha* mutants, do not distinguish between these possibilities. Somatic mosaicism for *cha* or *ace* was generated specifically in the eye by mitotic recombination induced by an *eyeless* enhancer-driven FLP recombinase (12, 13). In addition, a positive marking system (27) was used to label mutant axons by the expression of membrane-targeted GFP.

When the frequency of homozygous *cha* or *ace* mutant photoreceptor neurons was low, mutant photoreceptor axon projections appeared normal (data not shown). However, with a *Minute* mutation or a cell-lethal mutation in trans to *cha* or *ace*, retinas with a large proportion of the homozygous mutant cells were recovered. A phenotypic series was obtained by examining cha^{ts2} mosaic animals after growth at different temperatures. Photoreceptor axons projected normally into the optic lobe in animals raised at the permissive temperature. When grown at 28°C (a semipermissive temperature), ≈10% of the specimens (n = 240) with large cha^{ts2} clones displayed aberrant axon projection phenotypes. Although the photoreceptor axons entered the optic stalk normally, they sometimes behaved abnormally at the exit, and in rare cases formed ectopic bundles that missed the lamina target field entirely. Mutant axons that entered the lamina established an uneven distribution, where the growth cones failed establish a continuous plexus layer composed of R1–R6 axon termini (Fig. 2 *c* and *c′*; see also Fig. 4*c*). Mutant growth cones sometimes sent out extensions over unusually long distances (arrow in Fig. 2 *c* and *c′*). At the nonpermissive temperature (30°C), specimens displayed similar, but more frequent and severe, defects (Fig. 2 *d* and *d′*; 75%, n = 120). However, *cha* loss-of-function did not prevent photoreceptor axons from discriminating between appropriate optic lobe target layers. When the axons of *cha* mutant photoreceptors R3 and R4 were specifically labeled (by use of *mδ-GAL4*; ref. 14), some extension of mutant growth cones beyond the lamina plexus was observed (Fig. 2*g*), but these axons did not extend into the medulla target field.

Lamina neuronal differentiation and glial migration into the lamina target field depend on signals delivered to the lamina by the photoreceptor axons (reviewed in ref. 28). Loss of *cha* activity did not affect either of these two processes, as indicated by the presence of normal numbers of neurons and glia. However, the position of these cells lacked normal layer-specific precision. Lamina neurons establish five neuron "cartridge" groups composed of neurons L1–L5, where L5 neurons form a distinct proximal layer (Fig. 2*h*). Lamina glia are organized into several layers according to glial cell type, and can be distinguished by shape, size, and relative position (Fig. 4*f*). Although distinct glial and neuronal layers could be discerned in the *cha* mosaic specimen, their organization was less precise (Fig. 2 *i* and *d* and data not shown).

To determine whether these defects in the establishment of axon projections were manifested in disorganization of the adult visual system, late pupal stage *cha* mosaic animals were examined (Fig. 2 *j–o*). R1–R6 axon termini in the lamina are normally organized into a regular array of cartridge units consisting of six (R1–R6) photoreceptor axon termini and L-neuron axons (Fig. 2 *j*, *k*, and *n*). The R7 and R8 axons form a precise array in specific layers of the medulla. In *cha* mutant specimens (Fig. 2 *l* and *m*), photoreceptor axons were segregated properly into lamina and medulla layers, but the projections were somewhat disorganized within each layer (Fig. 2*m*) as is evident in high-resolution views of lamina cartridges (Fig. 2*o*). Thus, the disor-

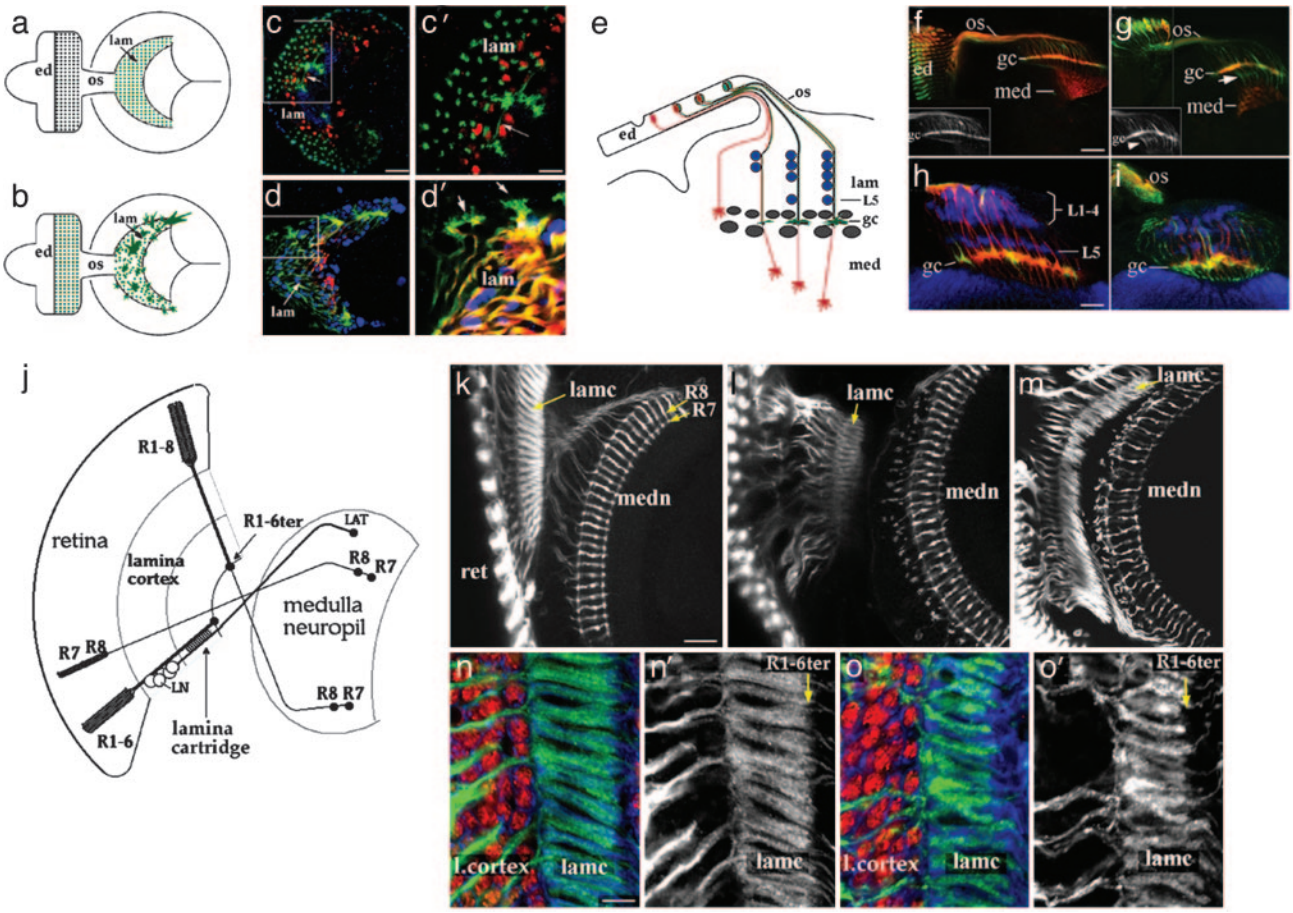

Fig. 2. Axon projection defects of photoreceptor neurons deprived of choline acyltransferase activity. (*a–d*) Mosaic animals with a high proportion of photoreceptor neurons homozygous for the cha^{ts2} (because of use of *Minute*; cha^{ts2}/cha^{ts2} positively marked by GFP; green) were raised at 28°C (*c* and *c′*) or 30°C (*d* and *d′*). In the wild type (*a*), ommatidia (green spots in the eye disk, ed) establish a one-to-one pattern of projections in the lamina (lam, green spots represent end-on views of axon fascicles). (*b*) The irregular axon behavior of a *cha* mosaic, with mutant growth cones extending profuse filopodia. (*c* and *c′*) At 28°C, *cha* mutant axons display defects occasionally, with growth cones extending branches over long distances (arrow in *c*, high-magnification view shown in *c′*). Lamina neurons are labeled by anti-Elav (red) in *c* and *c′*. (*d* and *d′*) At 30°C, the defects are more frequent and severe, with extensive filopodia emanating from *cha* mutant growth cones (arrows, high-magnification view in *d′*). Glia are labeled by anti-Repo (blue). (*e–i*) Correct layer targeting of *cha* mutant photoreceptor axons. (*e*) The horizontal perspective reveals the layered cellular organization of the developing lamina (lam). R1-R6 axons (green) terminate in the lamina plexus (gc) between two layers of glia (gray). Distal to the glial layers, lamina neurons L1-L5 (blue) form distinct layers, with an L5 layer located proximally. R7 and R8 axons (red) project through the lamina to the medulla (med). (*f–i*), The R3 and R4 neurons were labeled specifically (green) in cha^{ts2} mosaic specimens by use of the *mδ-GAL4* driver (14). In wild type (*f*), GFP-positive R3 and R4 axons (grayscale in the *Inset*) terminate in the lamina plexus layer (gc), whereas R7 and R8 axons (red; Mab24B10 labeling) extend to the medulla (med). In a *cha* mosaic maintained at 28°C (*g*), many GFP-positive growth cones extend beyond the plexus layer (white arrow), but not as far as R7 or R8 termini (labeling as in *f*). (*h*) Labeling of lamina neurons with anti-Elav (blue) reveals two distinct layers, visible in this wild-type specimen. In a corresponding cha^{ts2} mosaic specimen (*i*), these layers are present but irregular. (*j–o*). Consequences of *cha* loss-of-function for adult visual system connectivity. (*j*) In the adult visual system, R1–R6 axons (R1–6ter) and R7/R8 axons terminate retinotopically in the lamina and medulla, respectively. R1–R6 axons are distributed in a stereotyped pattern to ''cartridges,'' where they synapse with L-neurons. R7 and R8 axons terminate in distinct medulla target layers. (*k*) These features of connectivity are readily discernible in a wild-type specimen (photoreceptor axons labeled by Mab24B10). (*l* and *m*) In cha mosaic animals raised at the semipermissive (*l*) and nonpermissive (*m*) temperatures, cartridge structure (lamc) and R7, R8 terminal patterning are notably perturbed, especially at the nonpermissive temperature. (*n* and *o*) Effects of *cha* loss-of-function on lamina cartridge organization are readily visible in high-magnification views (*o* and *o′*), where photoreceptor axon terminals are labeled with Mab24B10 (green in *n* and *o*; grayscale in *n′* and *o′*), and lamina neurons are labeled by anti-Elav (red in *n* and *o*). *n* and *n′* show wild type. (Scale bars: 10 μm in *c* for *c* and *d*, 4 μm in *c′* for *c′* and *d′*, 10 μm in *f* for *f* and *g*, 5 μm in *h* for *h* and *i*, 15 μm in *k* for *k–m*, and 5 μm in *n* for *n*, *n′*, *o*, and *o′*.)

ganization within each target area that was noted at axon ingrowth was observed in the final pattern of synaptic connectivity.

Significant photoreceptor axon guidance defects were also observed in specimens harboring large retinal clones of the strong *ace* alleles, ace^{J50} and ace^{J21} (Fig. 3 *e* and *f*). In these animals, mutant axons wandered well off normal paths and/or crossed over aberrantly. These effects displayed some degree of local nonautonomy, as wild-type axons in the vicinity of *ace* axons also behaved aberrantly (e.g., the GFP-negative axons in Fig. 3*e*). As for *cha* mosaics, labeling R3/R4 axons specifically did not reveal significant mistargeting of these axons to the medulla layer (data not shown). Ommatidial development was also assessed and found to be normal (Fig. 3*d*). These results indicate that photoreceptor neurons require normal acetylcholine synthesis and metabolism for pathfinding by their growth cones.

As a neurotransmitter, acetylcholine utilizes the vesicular acetylcholine transporter protein (Vacht) to be packaged into synaptic vesicles and transported to the synapse (29). The functional dependence of acetylcholine export on Vacht is underscored by the cross-species conservation of acetylcholine gene loci, in which *cha* and *vacht* share a first exon, and *vacht* is

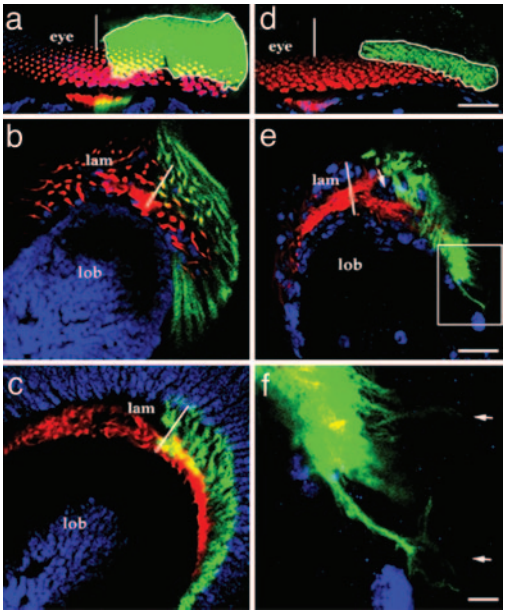

Fig. 3. Roles of acetylcholinesterase (Ace) and the vesicular acetylcholine transporter, Vacht, in photoreceptor axon guidance. Eye-specific mosaicism for *vacht*^{1} (*a*–*c*), *ace*^{J50} (*d*–*f*), and *ace*^{J21} (data not shown) was induced by using the positive marking system (GFP, green). The photoreceptor axons were also labeled by Mab24B10 (red), which labels older (posterior) photoreceptor neurons. Neurons are labeled by anti-Elav in *a*–*c* (blue), and glia are labeled in *d*–*f* by anti-Repo (blue). (*a*–*c*) *vacht*^{1} mutant photoreceptor neurons form normal ommatidia (*a*) and establish normal axon projections into the lamina (*b*) and medulla (*c*). (*d*–*f*) *ace*^{J50} ommatidia appear normal (*d*), but their photoreceptor axons project aberrantly (*e*), sending out multiple extensions visible in the high-magnification view of the boxed area (*e*) shown in *f* (arrows). In the lamina plexus layer, wild-type growth cones (red, GFP-negative) take up normal positions, whereas GFP-positive *ace*^{J50} axons fail to arborize, leaving a void (arrow in e). White lines mark the dorsoventral midline positions of the eye (*a* and *d*) or lamina (*b*, *c*, and *e*). (Scale bars: 15 μm in *d* for *d* and *a*, 15 μm in *e* for *b*, *c*, and *e*, and 3 μm in *f*.)

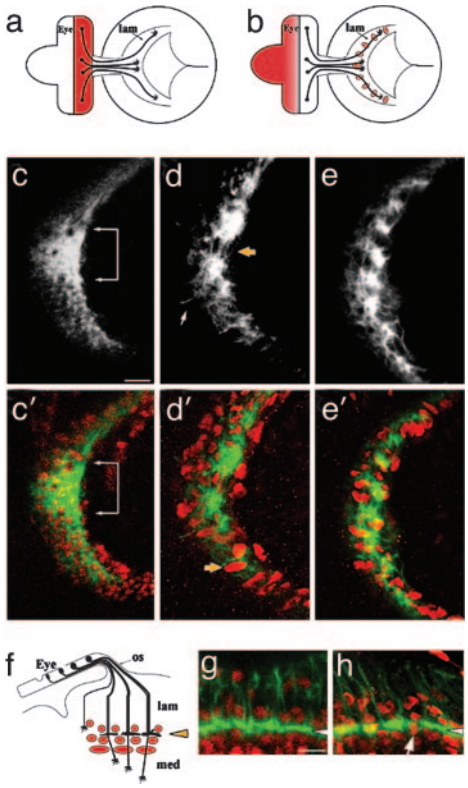

Fig. 4. Axon projection phenotype caused by expression of α-BGT. (*a*) Expression of *GMR-GAL4* (pink) in a late third-instar visual system. (*b*) Expression of *ey-GAL4* (pink) in the undifferentiated retinal field and lamina glia. (*c* and *c*′) The normal lamina plexus layer of a *GMR-GAL4* specimen. A focal plane that includes the R1–R6 growth cone plexus sheet (mAb24B10, grayscale in *c*, green in *c*′) is indicated by a white bracket. Lamina glia lie above and below the growth cone layer (red in *c*′, anti-Repo). (*d* and *d*′) *GMR-GAL4* driven *UAS-α-BGT* disrupts the growth cone plexus layer (yellow arrow in d), and causes mis-positioning of lamina glia. A marginal glial cell is mis-positioned distally (d′, yellow arrow). A white arrow indicates an aberrant axonal projection. Antibody labeling as in *c* and *c*′. (e and e′) *ey-GAL4*-driven *UAS-αBGT* expression results in a defect like that observed with the *GMR-GAL4* driver (*d* and *d*′). Antibody labeling as in *c* and *c*′. (*f*) The layered pattern of lamina glia above (epithelial) and below (marginal, medulla) the R1–R6 growth cone terminations in the lamina plexus. (*g*) A horizontal view of *mδ-GAL4*-driven GFP expression, showing the region in *f*. The arrowhead indicates the plexus layer, labeled by *mδ-GAL4*-driven GFP expression (green). Glia (red, anti-Repo) lie above and below this layer. (*h*) An *mδ-GAL4*, *UAS-CD8::GFP*; *UAS-α-BGT* specimen, labeled and viewed as in *g*. Note that the plexus layer (white arrow) is disrupted by glia extending through it, and the additional mis-positioning of glia throughout the lamina. (Scale bars: 10 μm in *c* for *c*–*e* and 5 μm in *g* for *g* and *h*.)

located in the first intron of the *cha* locus (23, 30). To test the notion that a transporter-mediated accumulation of acetylcholine is required for its activity in retinal axon navigation, photoreceptor cells lacking Vacht were generated in mosaic animals by use of the method described for *cha* and *ace* above. Photoreceptor axons were found to project normally in these animals (Fig. 3 *a*–*c*). Consistent with the notion that a synaptic vesicle pathway is not involved in the delivery of acetylcholine during photoreceptor axon pathfinding, transgenic expression of the tetanus toxin light chain (31) in photoreceptor neurons did not yield a defect in the projection pattern of photoreceptor axon termini in the lamina. These observations indicate that the developmental role of acetylcholine in the visual system does not require its release by a mechanism dependent on synapse formation or neural activity.

Studies in culture have implicated nAChRs in mediating acetylcholine's effects on growth cone behavior, and shown that these effects coincide with calcium influx (7, 32). We sought to address the question of whether nAChRs were mediating acetylcholine's effect on *Drosophila* photoreceptor axons as well. First, we examined the expression and axonal localization of nAChR subunits for which there are available antibody reagents. We found that two α subunits, Dα2 (33) and ALS (34), are concentrated on photoreceptor axons during their ingrowth into the brain (Fig. 1*d* and data not shown). Biochemically, these two α subunits can be found localized in the same nAChR complexes in extracts of *Drosophila* head (35).

There are no mutants known for any of the 11 known nAChR subunit genes of *Drosophila* (36). Moreover, because there are multiple genes for each subunit type, mutation of a single subunit gene might not suffice to abolish receptor activity. Therefore, we decided to make use a natural antagonist of nAChR. It has been demonstrated that the small protein toxin α-BGT binds specifically to the nAChR and blocks neurotransmission by acetylcholine in *Drosophila* (37) as in vertebrates. We used a synthetic α-BGT gene (15) to generate transgenic flies that could express α-BGT under the control of the UAS promoter. The *GAL4* drivers *GMR-GAL4* (17), *eyeless-GAL4*, and *mδ-GAL4* (14) were used to express the *α-BGT* transgene in the developing visual system. *GMR-GAL4* expression is specific to the developing retina and commences shortly after the photoreceptor cells begin differentiation (Fig. 4*a*). *ey-GAL4*, a construct based on the *eyeless* gene promoter, drives expression in the undifferentiated

photoreceptor precursor field and confers strong *GAL4* expression in a subset of lamina glial cells, where secretion of α-BGT would also possibly act directly on photoreceptor axon termini or lamina cells (Fig. 4*b*). As noted above, the *mδ-GAL4* driver is expressed in the photoreceptors R3 and R4 (14). These *GAL4* drivers, by themselves, did not affect axon projections and the distribution of growth cones with the lamina plexus (e.g., Fig. 4*c*; animals raised at 25°C). In contrast, the expression of α-BGT disrupted the photoreceptor axon projection pattern (Fig. 4 *d*, *e*, and *h*) in a manner reminiscent of the semipermissive temperature phenotypes observed in *cha* mosaic animals. Axon fascicles formed abnormal associations, resulting in unusually large and uneven bundles, instead of the normal continuous R1–R6 growth cone plexus layer (Fig. 4*c*). Expression of α-BGT specifically in R3 and R4 neurons (with *mδ-GAL4*) did not prevent the axons from terminating in the lamina (Fig. 4*h*). However, some disorganization of the cellular components of the lamina was observed. Epithelial and marginal glia normally form layers above and below, respectively, the R1–R6 growth cone plexus (Fig. 4 *f* and *g*). Notably, these glia were not confined to their proper layers (arrow in Fig. 4*d′*) and could be found extending through the growth cone plexus (arrow in Fig. 4*h*).

We suppose that the relatively mild phenotypes, in comparison to the effects of strong disruption of acetylcholine metabolism, could be due to only partial interference in nicotinic receptor activity by α-BGT expression, or to only a partial reliance of signaling on α-BGT-sensitive receptors. Indeed, animals that expressed a single copy of the α-BGT transgene ubiquitously under control of a moderately strong neural-specific *GAL4* driver *elav-GAL4* were viable and fertile, and exhibited no obvious behavioral abnormalities. Thus, the transgenic α-BGT expression is not sufficiently disruptive to ACh signaling so as to produce gross effects on viability or behavior.

Discussion

We have found that the establishment of the precise fine structure of photoreceptor axon projections in the *Drosophila* visual system depends on the synthesis and reception of the transmitter acetylcholine. Acetylcholine was detected on photoreceptor axons and in their target field in a pattern consistent with secretion from the photoreceptor axon terminals. Retinal axon projections were perturbed when either of two enzymes involved in acetylcholine metabolism, ChAT or AChE, was specifically eliminated from developing photoreceptor cells. The tendency for larger populations of *cha* or *ace* mutant neurons to manifest more severe axon projection defects suggests a non-cell autonomous effect of acetylcholine, which could be mediated by the local diffusion of acetylcholine away from axon termini. Perturbation of acetylcholine signaling via transgenic expression of α-BGT, which binds to and inhibits *Drosophila* nAChRs (37), resulted in axon projection defects similar to those observed in *cha* and *ace* mutants. The preferential expression of two nAChR subunits Dα2 and ALS on photoreceptor axons suggests that acetylcholine may have an autocrine or paracrine role in regulating the response of photoreceptor growth cones to guidance cues in the brain. However, because α-BGT is a nonautonomous inhibitor, whether the photoreceptor cells directly require cholinergic reception remains to be determined. All of these perturbations of acetylcholine signaling primarily affected the local fine structure of axonal connectivity within optic lobe target areas, rather than in the axon's choice of target layer.

It has been suggested by culture studies that calcium influx into the growth cone might mediate the action of acetylcholine-activated nicotinic receptors (7, 32, 38) or glutamate-activated α-amino-3-hydroxy-5-methyl-4-isoxazolepropionic acid/kainate receptors (39). In fact, cytosolic calcium has emerged as an important second messenger regulating growth cone structure and behavior (40, 41); calcium spikes induced by acetylcholine in cultured neurites have been shown to enhance cell–cell adhesion among growth cones and between growth cones and acetylcholine receptor-rich sensory neurons (42). Intriguingly, the growth cones of developing *Drosophila* retinal axons are initially blunt-tipped as they travel through the optic stalk. Upon reaching the lamina, the growth cones of R1–R6 axons expand in a stepwise manner to extend filopodia (18). One can interpret the filopodia-rich morphology of isolated *cha* or *ace* mutant growth cones as an indication that acetylcholine may be required to inhibit a precocious switch of the growth cone from the "blunt" mode to the filopodia-extending mode, or to in some other manner regulate the latter state.

The distinction between synaptic and developmental functions of acetylcholine is underscored by the observation that this developmental role of acetylcholine does not require the vesicular acetylcholine transporter protein, Vacht (Fig. 3 *a–c*), which is required for acetylcholine synaptic transmission. The release of acetylcholine from photoreceptor axons might, thus, use the general secretory pathway and be distributed via a nonvesicular mechanism, as has been observed in other systems (43–47). Spontaneous acetylcholine secretion from developing growth cones of *Drosophila* can be blocked by the nicotinic receptor antagonist curare and by α-BGT, but not by tetrodotoxin (6), which specifically blocks nerve-evoked synaptic transmission. This observation is consistent with an early role of acetylcholine in the establishment of axon projections that does not use an activity-dependent vesicle-mediated mode of delivery. It has also been shown that nonvesicular glutamate release results in the down-regulation of postsynaptic glutamate receptor field size (48), and that, in CA1 hippocampal neurons of embryonic and neonatal stage in rats, early release of γ-aminobutyric acid and glutamate does not require action potential, Ca^{2+} influx, or the soluble *N*-ethylmaleimide-sensitive factor attachment protein receptor complex (3).

A number of genetic studies on the acetylcholine pathway have been published. Disruptions in acetylcholine metabolism cause disorders affecting the neuromuscular junction (NMJ) in human (49), *Caenorhabditis elegans* (50), and the mouse (51), as well as defects in the structure and function of the *Drosophila* CNS (25, 52–54). The NMJ phenotypes observed in *C. elegans* and mouse include increased axonal branching and sprouting. These studies could not establish that acetylcholine exerted a direct effect on axons before synapse formation because acetylcholine was removed in the whole animal, not specific tissues. Nor could it be determined whether acetylcholine is required as anything other than a neurotransmitter. In the case of human myasthenic syndrome, the temporal and spatial distribution of acetylcholine coincides with its role as a transmitter delivered during synaptic activity (49). In the case of *C. elegans*, the phenotype of acetylcholine deficiency can be mimicked by mutations that block activity of the synaptic transmission machinery (50). Similar roles have been found for other neurotransmitters, including serotonin, dopamine, and glutamate (55–61). It is worth noting that, in the mammalian CNS, synapse maintenance, rather than synapse formation, depends on synaptic transmission (62). The early effect on axon behavior we have observed by eliminating acetylcholine, on the other hand, is clearly distinct from the role acetylcholine assumes at the synapse, a point underscored by the fact that acetylcholine is not synthesized by mature photoreceptors, which use histamine as the transmitter for phototransduction (8, 9). Our data present clear evidence for an early and somewhat unconventional role of acetylcholine *in vivo* in the initial formation of projection pattern of photoreceptor axons.

We are grateful to J. Hall (Brandeis University, Waltham, MA), P. Salvaterra (Beckman Research Institute of the City of Hope, Duarte, CA), T. Kitamoto (Beckman Research Institute of the City of Hope,

Duarte, CA), E. Gundelfinger (University of Hohenheim, Stuttgart), T. Rosenberry (Mayo Clinic, Jacksonville, FL), C. O'Kane (Cambridge University, Cambridge, U.K.), P. Garrity (Massachusetts Institute of Technology, Cambridge), S. Sweeney (Cambridge University, Cambridge, U.K.), B. Ganetzky (University of Wisconsin, Madison), H. Keshishian (Yale University, New Haven, CT), R. Hardie (Cambridge University, Cambridge, U.K.), C. Zuker (University of California at San Diego, La Jolla), Y. Zhong (Cold Spring Harbor Laboratory, Cold Spring Harbor, NY), L. Luo (Stanford University, Stanford, CA), M. Domínguez (Universität Zürich, Zürich), E. Hafen (Universität Zürich, Zürich), and E. Hawrot (Brown Medical School, Providence, RI) for strains and reagents; G. Leitinger for technical advice; and T. Wozniak and J. Jeong for technical assistance. This work was supported by National Institutes of Health (NIH)/National Eye Institute Grant EY10112 (to S.K.) and a NIH predoctoral training grant in Genetics (to H.Y.).

1. Nguyen, L., Rigo, J. M., Rocher, V., Belachew, S., Malgrange, B., Rogister, B., Leprince, P. & Moonen, G. (2001) *Cell Tissue Res.* **305,** 187–202.
2. Owens, D. F. & Kriegstein, A. R. (2002) *Nat. Rev. Neurosci.* **3,** 715–727.
3. Demarque, M., Represa, A., Becq, H., Khalilov, I., Ben-Ari, Y. & Aniksztejn, L. (2002) *Neuron* **36,** 1051–1061.
4. Young, S. H. & Poo, M. M. (1983) *Nature* **305,** 634–637.
5. Hume, R. I., Role, L. W. & Fischbach, G. D. (1983) *Nature* **305,** 632–634.
6. Yao, W. D., Rusch, J., Poo, M. & Wu, C. F. (2000) *J. Neurosci.* **20,** 2626–2637.
7. Zheng, J. Q., Felder, M., Connor, J. A. & Poo, M. M. (1994) *Nature* **368,** 140–144.
8. Sarthy, P. V. (1991) *J. Neurochem.* **57,** 1757–1768.
9. Burg, M. G., Sarthy, P. V., Koliantz, G. & Pak, W. L. (1993) *EMBO J.* **12,** 911–919.
10. Kunes, S., Wilson, C. & Steller, H. (1993) *J. Neurosci.* **13,** 752–767.
11. Rind, F. C. & Leitinger, G. (2000) *J. Comp. Neurol.* **423,** 389–401.
12. Newsome, T. P., Asling, B. & Dickson, B. J. (2000) *Development (Cambridge, U.K.)* **127,** 851–860.
13. Stowers, R. S. & Schwarz, T. L. (1999) *Genetics* **152,** 1631–1639.
14. Neves, G., Zucker, J., Daly, M. & Chess, A. (2004) *Nat. Genet.* **36,** 240–246.
15. Levandoski, M. M., Caffery, P. M., Rogowski, R. S., Lin, Y., Shi, Q. L. & Hawrot, E. (2000) *J. Neurochem.* **74,** 1279–1289.
16. Brand, A. H. & Perrimon, N. (1993) *Development (Cambridge, U.K.)* **118,** 401–415.
17. Freeman, M. (1996) *Cell* **87,** 651–660.
18. Meinertzhagen, I. A. & Hanson, I. (1993) in *The Development of Drosophila melanogaster*, eds. Bate, M. & Martinez-Arias, A. (Cold Spring Harbor Lab. Press, Plainview, NY), pp. 1363–1491.
19. Yasuyama, K., Kitamoto, T. & Salvaterra, P. M. (1995) *Cell Tissue Res.* **282,** 193–202.
20. Wolfgang, W. J. & Forte, M. A. (1989) *Dev. Biol.* **131,** 321–330.
21. Salvaterra, P. M. & McCaman, R. E. (1985) *J. Neurosci.* **5,** 903–910.
22. Takagawa, K. & Salvaterra, P. (1996) *Neurosci. Res.* **24,** 237–243.
23. Kitamoto, T., Xie, X., Wu, C. F. & Salvaterra, P. M. (2000) *J. Neurobiol.* **42,** 161–171.
24. Zador, E. (1989) *Mol. Gen. Genet.* **218,** 487–490.
25. Greenspan, R. J., Finn, J. A., Jr., & Hall, J. C. (1980) *J. Comp. Neurol.* **189,** 741–774.
26. Schumacher, M., Camp, S., Maulet, Y., Newton, M., MacPhee-Quigley, K., Taylor, S. S., Friedmann, T. & Taylor, P. (1986) *Fed. Proc.* **45,** 2976–2981.
27. Lee, T. & Luo, L. (1999) *Neuron* **22,** 451–461.
28. Kunes, S. (2000) *Curr. Opin. Neurol.* **10,** 58–62.
29. Gasnier, B. (2000) *Biochimie* **82,** 327–337.
30. Kitamoto, T., Wang, W. & Salvaterra, P. M. (1998) *J. Biol. Chem.* **273,** 2706–2713.
31. Sweeney, S. T., Broadie, K., Keane, J., Niemann, H. & O'Kane, C. J. (1995) *Neuron* **14,** 341–351.
32. Edwards, J. A. & Cline, H. T. (1999) *J. Neurophysiol.* **81,** 895–907.
33. Jonas, P. E., Phannavong, B., Schuster, R., Schroder, C. & Gundelfinger, E. D. (1994) *J. Neurobiol.* **25,** 1494–1508.
34. Schuster, R., Phannavong, B., Schroder, C. & Gundelfinger, E. D. (1993) *J. Comp. Neurol.* **335,** 149–162.
35. Schulz, R., Bertrand, S., Chamaon, K., Smalla, K. H., Gundelfinger, E. D. & Bertrand, D. (2000) *J. Neurochem.* **74,** 2537–2546.
36. Adams, M. D., Celniker, S. E., Holt, R. A., Evans, C. A., Gocayne, J. D., Amanatides, P. G., Scherer, S. E., Li, P. W., Hoskins, R. A., Galle, R. F., *et al.* (2000) *Science* **287,** 2185–2195.
37. Dudai, Y. (1977) *FEBS Lett.* **76,** 211–213.
38. Zheng, J. Q., He, X. P., Yang, A. Z. & Liu, C. G. (2000) *Acta Pharmacol. Sin.* **21,** 1016–1020.
39. Chang, S. & De Camilli, P. (2001) *Nat. Neurosci.* **4,** 787–793.
40. Gomez, T. M. & Spitzer, N. C. (2000) *J. Neurobiol.* **44,** 174–183.
41. Spitzer, N. C. (2002) *J. Physiol. (Paris)* **96,** 73–80.
42. Tatsumi, H. & Katayama, Y. (1999) *Neuroscience* **92,** 855–865.
43. Katz, B. & Miledi, R. (1977) *Proc. R. Soc. London Ser. B* **196,** 59–72.
44. Honmou, O., Kocsis, J. D. & Richerson, G. B. (1995) *Epilepsy Res.* **20,** 193–202.
45. Descarries, L., Gisiger, V. & Steriade, M. (1997) *Prog. Neurobiol.* **53,** 603–625.
46. Jabaudon, D., Shimamoto, K., Yasuda-Kamatani, Y., Scanziani, M., Gahwiler, B. H. & Gerber, U. (1999) *Proc. Natl. Acad. Sci. USA* **96,** 8733–8738.
47. Sharma, G. & Vijayaraghavan, S. (2002) *J. Neurobiol.* **53,** 524–534.
48. Featherstone, D. E., Rushton, E. & Broadie, K. (2002) *Nat. Neurosci.* **5,** 141–146.
49. Ohno, K., Tsujino, A., Brengman, J. M., Harper, C. M., Bajzer, Z., Udd, B., Beyring, R., Robb, S., Kirkham, F. J. & Engel, A. G. (2001) *Proc. Natl. Acad. Sci. USA* **98,** 2017–2022.
50. Zhao, H. & Nonet, M. L. (2000) *Development (Cambridge, U.K.)* **127,** 1253–1266.
51. Misgeld, T., Burgess, R. W., Lewis, R. M., Cunningham, J. M., Lichtman, J. W. & Sanes, J. R. (2002) *Neuron* **36,** 635–648.
52. Chase, B. A. & Kankel, D. R. (1988) *Dev. Biol.* **125,** 361–380.
53. Hall, J. C., Greenspan, R. J. & Kankel, D. R. (1979) in *Aspects of Developmental Neurobiology*, ed. Ferrendelli, J. A. & Gurvitch, G. (Soc. Neurosci. Press, Bethesda), pp. 1–42.
54. Greenspan, R. J. (1980) *J. Comp. Physiol.* **137,** 83–92.
55. Haydon, P. G., McCobb, D. P. & Kater, S. B. (1987) *J. Neurobiol.* **18,** 197–215.
56. Mattson, M. P. (1988) *Brain Res.* **472,** 179–212.
57. McCobb, D. P. & Kater, S. B. (1988) *Dev. Biol.* **130,** 599–609.
58. McCobb, D. P., Cohan, C. S., Connor, J. A. & Kater, S. B. (1988) *Neuron* **1,** 377–385.
59. McCobb, D. P., Haydon, P. G. & Kater, S. B. (1988) *J. Neurosci. Res.* **19,** 19–26.
60. Goldberg, J. I. & Kater, S. B. (1989) *Dev. Biol.* **131,** 483–495.
61. Mazer, C., Muneyyirci, J., Taheny, K., Raio, N., Borella, A. & Whitaker-Azmitia, P. (1997) *Brain Res.* **760,** 68–73.
62. Verhage, M., Maia, A. S., Plomp, J. J., Brussaard, A. B., Heeroma, J. H., Vermeer, H., Toonen, R. F., Hammer, R. E., van den Berg, T. K., Missler, M., *et al.* (2000) *Science* **287,** 864–869.